Multivariate GNSS Attitude Integrity: The Role of Affine Constraints

Gabriele Giorgi and Peter J.G. Teunissen

Abstract

In this work we analyze the integrity properties of an affine-constrained estimator applied to arrays of GNSS antennas. GNSS pseudorange and carrier phase measurements from multiple antennas whose relative positions are known are cast in a linearly-constrained observation model. The linear constraints are inherent to an affine transformation that is applied to the baseline coordinates. The affine transformation yields enhanced redundancy, thus improving the model integrity properties with respect to the unconstrained model. The extent of the improvement is measured in terms of internal and external reliability.

Keywords

Affine constrained attitude model • Attitude determination • Galileo • GNSS • GPS • ILS • MDB • Multivariate ILS • Reliability

1 Introduction

GNSS carrier phase attitude determination enables precise estimations of a body orientation in space, see e.g. Bar-Itzhack et al. (1998), Cohen (1992) and Giorgi (2011). In order to derive the orientation of the body with respect to a reference frame, an array of GNSS antennas is employed. The distances between antennas are surveyed a priori, such that the coordinates of each baseline are known in a local reference frame (e.g., a frame integral with the body). The estimation of the orientation of the local frame with respect to the frame in which the GNSS measurements are expressed is the aim of attitude determination.

Carrier phase-based attitude estimations are characterized by a much higher estimation precision than code-only processing, but the carrier phase measurements are inherently ambiguous by an unknown number of integer cycles (Strang and Borre 1997; Teunissen and Kleusberg 1998). These have to be resolved to their correct integer value. Application of Integer Least-Squares (ILS) to resolve the integer ambiguities guarantees the highest possible success rate among the admissible integer estimators, see Teunissen (1993) and Teunissen (1999). ILS methods have been recently studied in the context of nonlinear constrained models such as the GNSS-based attitude estimation problem (Giorgi 2011; Giorgi et al. 2012; Teunissen 2007). The baselines formed by the GNSS antenna array can be re-parameterized in terms of an attitude matrix. An admissible attitude matrix is orthonormally-constrained (OC) (Shuster 1993). If these constraints are integrated in the estimation of the whole parameter space, i.e., the attitude matrix and the integer ambiguities, a nonlinear estimation problem has to be solved. It is shown in Giorgi et al. (2011) and Teunissen (2007) how to solve for the OC GNSS attitude model, and it is demonstrated how the rigorous inclusion of the orthonormality constraint largely enhances ambiguity resolution.

A model of intermediate strength between the unconstrained (UC) and the OC approaches is obtained by operating the re-parameterization of the baselines in terms of

G. Giorgi (✉)
Institute for Communications and Navigation, Technische Universität München, München, Germany
e-mail: gabriele.giorgi@tum.de

P.J.G. Teunissen
Global Navigation Satellite Systems Research Centre, Curtin University of Technology, Perth, Australia
e-mail: P.Teunissen@curtin.edu.au

International Association of Geodesy Symposia,
DOI 10.1007/1345_2015_1,

the attitude matrix, but neglecting the associated nonlinear constraints. This yields an affine-constrained (AC) GNSS attitude model, as introduced in Giorgi and Teunissen (2013) and Teunissen (2012). This model has the advantage that it avoids the computational complexity of the OC GNSS attitude model, while it still has a significantly improved ambiguity resolution performance over its unconstrained counterpart.

More than improving the ambiguity resolution performances, the AC attitude model is characterized by enhanced integrity properties with respect to the UC model. Due to the affine-transformation of a parameter subset, a larger observations-to-unknowns redundancy enables smaller minimum detectable biases (MDBs), i.e., the minimum bias magnitude that can be detected, and smaller bias-to-noise ratios (BNRs), i.e., a measure of the influence of undetected errors on the parameter estimation. The MDBs and BNRs are used to measure the internal and external reliability of the observation model, respectively. It is shown in this contribution the impact that adopting the AC model over the UC model has on the model integrity properties.

This contribution is structured as follows. Section 2 introduces a theorem on the integrity properties of affine-constrained linear models.

Section 3 formulates the GNSS functional and stochastic model in multivariate form, for one-, two- and three-dimensional antenna arrays, tracking GNSS signals on an arbitrary number of frequencies with two or more antennas.

Section 4 analyzes the impact of the affine constraints on the model internal and external reliability. The MDBs and BNRs are given in analytical form, and the difference between the UC and AC approaches is analyzed from a theoretical as well as a numerical standpoint.

2 Reliability and Constraints: A Theorem

The Minimal Detectable Bias (MDB) and the Bias-to-Noise-Ratio (BNR) are two important diagnostic measures that describe the model reliability after statistical testing, see Baarda (1968) and Teunissen (2006). Let the m-vector of observables y be distributed under the hypothesis $\mathcal{H}$ as $y \sim \mathrm{N}(\mathrm{E}(y|\mathcal{H}), Q_{yy})$, and consider the null-hypothesis $\mathcal{H}_{\mathrm{U}}^0$ and the alternative hypothesis $\mathcal{H}_{\mathrm{U}}^a$,

$$\mathrm{E}(y|\mathcal{H}_{\mathrm{U}}^0) = Ax \quad \text{and} \quad \mathrm{E}(y|\mathcal{H}_{\mathrm{U}}^a) = Ax + c_y\nabla \tag{1}$$

in which $A \in \mathbb{R}^{m\times n}$ and $c_y \in \mathbb{R}^m$ are given (full rank) matrices, and x and ∇ are unknown parameters. The suffix 'U' has been used to discriminate this pair of hypotheses from their constrained counterparts, $\mathcal{H}_{\mathrm{C}}^o$ and $\mathcal{H}_{\mathrm{C}}^a$, respectively (see 3).

In Chapter 4 of Teunissen (2006) it is shown that the MDB and BNR of uniformly most powerful invariant (UMPI) testing $\mathcal{H}_{\mathrm{U}}^0$ against $\mathcal{H}_{\mathrm{U}}^a$ are given as

$$\begin{aligned} \mathrm{MDB}_{\mathrm{U}} &= \sqrt{\frac{\lambda_0}{||P_A^\perp c_y||^2_{Q_{yy}}}}, \\ \mathrm{BNR}_{\mathrm{U}} &= \mathrm{MDB}_{\mathrm{U}}\ ||P_A c_y||_{Q_{yy}} \end{aligned} \tag{2}$$

with noncentrality parameter λ_0, the weighted squared-norm $||.||^2_{Q_{yy}} = (.)^T Q_{yy}^{-1}(.)$ and the orthogonal projector $P_A = A(A^T Q_{yy}^{-1} A)^{-1} A^T Q_{yy}^{-1}$.

The following theorem shows how the MDBs and BNRs change when both the null- and alternative hypothesis are strengthened with the same constraints.

Theorem (Constraints, MDBs and BNRs) *Let the hypotheses of (1) be constrained as*

$$\begin{aligned} \mathrm{E}(y|\mathcal{H}_{\mathrm{C}}^0) &= Ax, & K^T x &= 0 \\ \mathrm{E}(y|\mathcal{H}_{\mathrm{C}}^a) &= Ax + c_y\nabla, & K^T x &= 0 \end{aligned} \tag{3}$$

with given full rank constraint matrix $K \in \mathbb{R}^{n\times p}$ $(p \le n)$. Then the unconstrained MDBs and BNRs of (1) are related to their constrained counterparts of (3) as

$$\frac{\mathrm{MDB}_{\mathrm{U}}^2}{\mathrm{MDB}_{\mathrm{C}}^2} = 1 + \frac{||P_L^\perp c_{\hat{x}}||^2_{Q_{\hat{x}\hat{x}}}}{||P_A^\perp c_y||^2_{Q_{yy}}} \tag{4}$$

$$\frac{\mathrm{BNR}_{\mathrm{U}}^2}{\mathrm{BNR}_{\mathrm{C}}^2} = \frac{\mathrm{MDB}_{\mathrm{U}}^2}{\mathrm{MDB}_{\mathrm{C}}^2}\left[1 - \frac{||P_L^\perp c_{\hat{x}}||^2_{Q_{\hat{x}\hat{x}}}}{||P_A c_y||^2_{Q_{yy}}}\right]^{-1} \tag{5}$$

with basis matrix L spanning the null space of K^T, and

$$\begin{aligned} P_L^\perp &= I - L(L^T Q_{\hat{x}\hat{x}}^{-1} L)^{-1} L^T Q_{\hat{x}\hat{x}}^{-1} \\ &= Q_{\hat{x}\hat{x}} K (K^T Q_{\hat{x}\hat{x}} K)^{-1} K^T \\ c_{\hat{x}} &= Q_{\hat{x}\hat{x}} A^T Q_{yy}^{-1} c_y \\ Q_{\hat{x}\hat{x}} &= (A^T Q_{yy}^{-1} A)^{-1} \end{aligned} \tag{6}$$

Proof From the definition of the MDB and its geometric interpretation (Teunissen 2006), we have

$$\frac{\mathrm{MDB}_{\mathrm{U}}^2}{\mathrm{MDB}_{\mathrm{C}}^2} = \frac{||P_{AL}^\perp c_y||^2_{Q_{yy}}}{||P_A^\perp c_y||^2_{Q_{yy}}} = 1 + \frac{(||P_A c_y||^2_{Q_{yy}} - ||P_{AL} c_y||^2_{Q_{yy}})}{||P_A^\perp c_y||^2_{Q_{yy}}} \tag{7}$$

With

$$\begin{aligned} Q_{\hat{x}\hat{x}} &= (A^T Q_{yy}^{-1} A)^{-1} \\ P_A &= A Q_{\hat{x}\hat{x}} A^T Q_{yy}^{-1} \\ P_{AL} &= AL(L^T Q_{\hat{x}\hat{x}}^{-1} L)^{-1} L^T A^T Q_{yy}^{-1} \\ P_L &= L(L^T Q_{\hat{x}\hat{x}}^{-1} L)^{-1} L^T Q_{\hat{x}\hat{x}}^{-1} \end{aligned} \tag{8}$$

it follows that

$$\begin{aligned} |P_A c_y||^2_{Q_{yy}} &= ||c_{\hat{x}}||^2_{Q_{\hat{x}\hat{x}}} \\ ||P_{AL} c_y||^2_{Q_{yy}} &= ||P_L c_{\hat{x}}||^2_{Q_{\hat{x}\hat{x}}} \end{aligned} \tag{9}$$

Substitution of (9) into (7) proves the result. The derivation of the BNR-ratio goes along similar lines. □

This theorem shows how the MDBs and BNRs improve (i.e. get smaller) when constraints are added to both the null- and alternative hypothesis. Such improvement will be absent if $||P_L^{\perp} c_{\hat{x}}||^2_{Q_{\hat{x}\hat{x}}} = 0$, i.e. if $c_{\hat{x}} = 0$ or $P_L^{\perp} c_{\hat{x}} = 0$. The first case occurs if the solution for x under $\mathcal{H}_{\mathrm{U}}^a$ is invariant for the modelling bias, i.e. when c_y is orthogonal to the range space of A. The second case occurs when $K^T c_{\hat{x}} = 0$, i.e. when the effect of the modeling bias on x is not felt in the constraint.

In the following we will apply the above theorem to the multivariate GNSS affine-constrained model.

3 Multivariate GNSS Observation Models

Consider an array of $r + 1$ GNSS antennas forming r independent baselines. The $2mf$ DD GNSS pseudorange and carrier phase observations obtained by simultaneously tracking $m + 1$ satellites on f frequencies, are cast in the columns of a $2mf \times r$ observation matrix Y. The DD multivariate UC GNSS observation model is formulated as

$$\begin{aligned} &\mathrm{E}(Y) = GB + NX \quad , \quad \mathrm{D}(\mathrm{vec}Y) = P \otimes Q_{yy} \\ &\text{with} \quad B \in \mathbb{R}^{3\times r} \ , \ X \in \mathbb{Z}^{mf\times r} \end{aligned} \tag{10}$$

The coordinates of the baselines forming the array are cast in the columns of matrix B, whereas X contains the integer-valued unknown ambiguities (the array is assumed small enough to neglect the atmospheric delays). The entries of the $2mf \times 3$ matrix G are the differenced line-of-sight vectors, and the $2mf \times mf$ matrix N contains the wavelengths.

The matrices P and Q_{yy} of the dispersion $\mathrm{D}(\mathrm{vec}Y)$ are given as $P = \frac{1}{2} D_r^T D_r = \frac{1}{2}(I_r + e_r e_r^T)$ and $Q_{yy} = 2\Sigma \otimes D_m^T D_m$, with cofactor matrices $\Sigma = \mathrm{blockdiag}[\Sigma_P, \Sigma_\Phi]$, $\Sigma_P = \mathrm{diag}\left(\sigma^2_{p_1}, \cdots, \sigma^2_{p_f}\right)$, $\Sigma_\Phi = \mathrm{diag}\left(\sigma^2_{\phi_1}, \cdots, \sigma^2_{\phi_f}\right)$ containing the undifferenced code and phase variances, and where $D_t^T = [-e_t, I_t]$ is an $t \times (t+1)$ differencing matrix.

We define a local frame in which the baseline coordinates are invariant, and introduce a $q \times r$ matrix F whose entries are the local baseline coordinates. Parameter q denotes the rank of matrix F: $q = 1$ for configurations of r antennas aligned in the same direction, $q = 2$ for configurations of r coplanar antennas and $q = 3$ for configurations of r non-coplanar antennas. The transformation between the local coordinate system and the reference system in which the observations are collected is defined by a rotation matrix R as

$$B = RF \quad ; \quad R \in \mathbb{O}^{3\times q} \ , \ F \in \mathbb{R}^{q\times r} \tag{11}$$

The attitude matrix belongs to the class of $3 \times r$ orthonormal matrices $\mathbb{O}$, i.e., matrix R fulfill the nonlinear constraints defined by $R^T R = I_q$. Substitution of relationship (11) into model (10) gives the OC attitude model:

$$\begin{aligned} &\mathrm{E}(Y) = GRF + NX \quad , \quad \mathrm{D}(\mathrm{vec}Y) = P \otimes Q_{yy} \\ &\text{with} \quad R \in \mathbb{O}^{3\times q} \ ; \ X \in \mathbb{Z}^{mf\times r} \end{aligned} \tag{12}$$

The solution of the OC model is inherently more complex than the UC model, due to the nonlinear constraints. The solution of model (12) has been given in Giorgi (2011), Giorgi et al. (2012), Giorgi et al. (2011), Teunissen (2007), and will not be discussed any further in this work.

A model of intermediate complexity is obtained by adopting the transformation (11), but disregarding the nonlinear constraints. The AC GNSS attitude model is then formulated as (Teunissen 2012)

$$\begin{aligned} &\mathrm{E}(Y) = GRF + NX \quad , \quad \mathrm{D}(\mathrm{vec}Y) = P \otimes Q_{yy} \\ &\text{with} \quad R \in \mathbb{R}^{3\times q} \ ; \ X \in \mathbb{Z}^{mf\times r} \end{aligned} \tag{13}$$

Hence, the orthonormality constraint $R \in \mathbb{O}^{3\times q}$ has been replaced by the constraint $R \in \mathbb{R}^{3\times q}$. Note that the transformation (11) allows to reduce the number of unknown parameters in (13) for those antenna configurations in which the span of the baselines is smaller than their number ($q < r$).

Since model (13) is linear, a classic ILS solution can be derived, as shown in Giorgi et al. (2011), Teunissen (2007) and Teunissen (2012).

3.1 Alternative Hypotheses

Models (10) and (13) will be treated as our null hypotheses $\mathcal{H}_{\mathrm{uc}}^0$ and $\mathcal{H}_{\mathrm{ac}}^0$, respectively. In order to check for errors and/or biases in the observation vector, or model misspecifications, we introduce two alternative functional models that will be compared to the representations (10) and (13). These alternative hypotheses are

$$\begin{aligned} &\mathcal{H}_{\mathrm{uc}}^a : \mathrm{E}(Y) = GB + NX + C\gamma, \quad \mathrm{D}(\mathrm{vec}Y) = P \otimes Q_{yy} \\ &\mathcal{H}_{\mathrm{ac}}^a : \mathrm{E}(Y) = GRF + NX + C\gamma, \ \mathrm{D}(\mathrm{vec}Y) = P \otimes Q_{yy} \end{aligned} \tag{14}$$

The scalar $\gamma \in \mathbb{R}$ denotes the error/bias magnitude, whereas matrix C defines the observation(s) affected by the error. We assume that matrix C can be expressed as the (outer) product between two vectors: $C = cd^T$, in which the $2mf$-vector c can be used to specify which observable is biased, and the r-vector d can be used to select the antenna of the biased observable. Thus, for instance, if the ith observable, of the

jth satellite, of the kth antenna is assumed biased, then c and d are chosen as $c = (I_{2f} \otimes D_m^T)(u_i^{2f} \otimes u_j^{m+1})$ and $d = D_r^T u_k^{r+1}$, in which u_i^n denotes a canonical unit vector of dimension n, with the 1 in its ith slot.

In the following section we analyze the integrity properties of the UC and AC observation models.

4 Integrity Properties

The MDBs and BNRs of models (10)–(13) tested against the corresponding alternative hypotheses in (14) follows from (2) as

$$\begin{aligned} MDB_{\text{uc}} &= \sqrt{\frac{\nu_0}{\sigma_{\hat{\gamma}_{\text{uc}}}^{-2}}} = \sqrt{\frac{\nu_0}{d^T P^{-1} d \bar{\bar{c}}_{N,\bar{G}}^T Q_{yy}^{-1} \bar{\bar{c}}_{N,\bar{G}}}} \\ BNR_{\text{uc}} &= MDB_{\text{uc}} \sqrt{d^T P^{-1} d \left(c^T Q_{yy}^{-1} P_N c + c^T Q_{yy}^{-1} P_{\bar{G}} c \right)} \end{aligned} \tag{15}$$

and

$$\begin{aligned} MDB_{\text{ac}} &= \sqrt{\frac{\nu_0}{\sigma_{\hat{\gamma}_{\text{ac}}}^{-2}}} = \sqrt{\frac{\nu_0}{\sigma_{\hat{\gamma}_{\text{uc}}}^{-2} + d^T P_S P^{-1} d \bar{c}_N^T P_{\bar{G}} \bar{c}_N}} \\ BNR_{\text{ac}} &= MDB_{\text{ac}} \\ &\quad \cdot \sqrt{d^T P^{-1} d c^T Q_{yy}^{-1} P_N c + d^T P_S^{\perp} P^{-1} d c^T Q_{yy}^{-1} P_{\bar{G}} c} \end{aligned} \tag{16}$$

with

$$\begin{aligned} \bar{\bar{c}}_{N,\bar{G}} &= [I - P_{\bar{G}}]\, \bar{c}_N = [I - P_{\bar{G}}][I - P_N]\, c \\ \bar{G} &= [I - P_N]\, G \\ P_{\bar{G}} &= \bar{G} \left[\bar{G}^T Q_{yy}^{-1} \bar{G} \right]^{-1} \bar{G}^T Q_{yy}^{-1} \\ P_N &= N \left[N^T Q_{yy}^{-1} N \right]^{-1} N^T Q_{yy}^{-1} \\ P_S &= I - P_S^{\perp} = I - P^{-1} F^T (F P^{-1} F^T)^{-1} F \end{aligned} \tag{17}$$

Matrix P_S is the projector of rank $r - q$ that projects onto the null space of the body frame baseline matrix F. This matrix reduces to the zero-matrix when the number of baselines r equals their span q.

Application of the Theorem given in Sect. 2 to the UC and AC observations models yields the following ratios between MDBs and between BNRs:

$$\omega = \frac{MDB_{\text{uc}}}{MDB_{\text{ac}}} = \sqrt{1 + \frac{d^T P_S P^{-1} d}{d^T P^{-1} d} \frac{\bar{c}_N^T Q_{yy}^{-1} P_{\bar{G}} \bar{c}_N}{\bar{c}_N^T Q_{yy}^{-1} P_{\bar{G}}^{\perp} \bar{c}_N}} \tag{18}$$

and

$$\tau = \frac{BNR_{\text{uc}}}{BNR_{\text{ac}}} = \frac{\omega}{\sqrt{1 - \frac{d^T P_S P^{-1} d c^T Q_{yy}^{-1} P_{\bar{G}} c}{d^T P^{-1} d \left(c^T Q_{yy}^{-1} P_N c + c^T Q_{yy}^{-1} P_{\bar{G}} c \right)}}} \tag{19}$$

with $P_{\bar{G}}^{\perp} = I - P_{\bar{G}}$. For $q = r$ the MDBs and BNRs of the two models UC and AC are equal. However, for $q < r$ the AC model is characterized by smaller MDBs and BNRs, or equivalently, the AC model is capable of detecting the same error magnitude with a larger power of detection. The extent of the improvement, quantified by the ratios ω and τ, depends on the number of baselines (r), their relative geometry (P_S), the measurement quality Q_{yy}, and the given satellite geometry distribution (G). Note that the ratios in (18)–(19) are independent from a geometrical scaling of the whole GNSS antenna array.

4.1 Numerical Example

We provide in this section a numerical example of the improvement obtained in terms of MDBs and BNRs ratios in two single-constellation case studies. We study both GPS and Galileo signals, assuming 4 to 10 satellites for each case, tracked on frequency L1, L2 and L5 (GPS), and E1-E5a-E5b-E5-E6 (Galileo), by an array of 4 coplanar antennas. The local baseline coordinates are

$$F = \begin{bmatrix} 1 & 0 & 0.5 \\ 0 & 1 & 1 \end{bmatrix} \tag{20}$$

The DD observation noise (Q_{yy}) is composed by using the variances reported in Table 1, and the GPS and Galileo simulated satellite positions are illustrated in the skyplots of Figs. 1 and 2. The DD observations are formed by differencing with respect to satellite '1'.

Table 2 reports several values of ratio ω as function of the number of satellites and channels (frequencies) tracked by the antenna array. We assume an error occurring on the third receiver, relative to a single satellite (first DD observation) on frequency L5. The improvement obtained with the AC GNSS model with respect to the UC model is rather large. In the weakest measurement scenario, i.e., only 5 satellites tracked on the single-frequency L5, the minimum detectable bias is twice as large for the UC model compared to the AC model. Stronger scenarios, i.e., higher number of satellites and/or multifrequency observations, are characterized by lower values, although in many cases sensibly larger than the unit.

Table 1 Standard deviations of GPS and Galileo undifferenced pseudorange and carrier phase (Φ) observables

	L1	L2	L5	E1	E5a	E5b	E5	E6
σ_P (cm)	25	25	15	20	15	15	7	15
σ_Φ (mm)	1.0	1.3	1.3	1.0	1.3	1.3	1.3	1.2

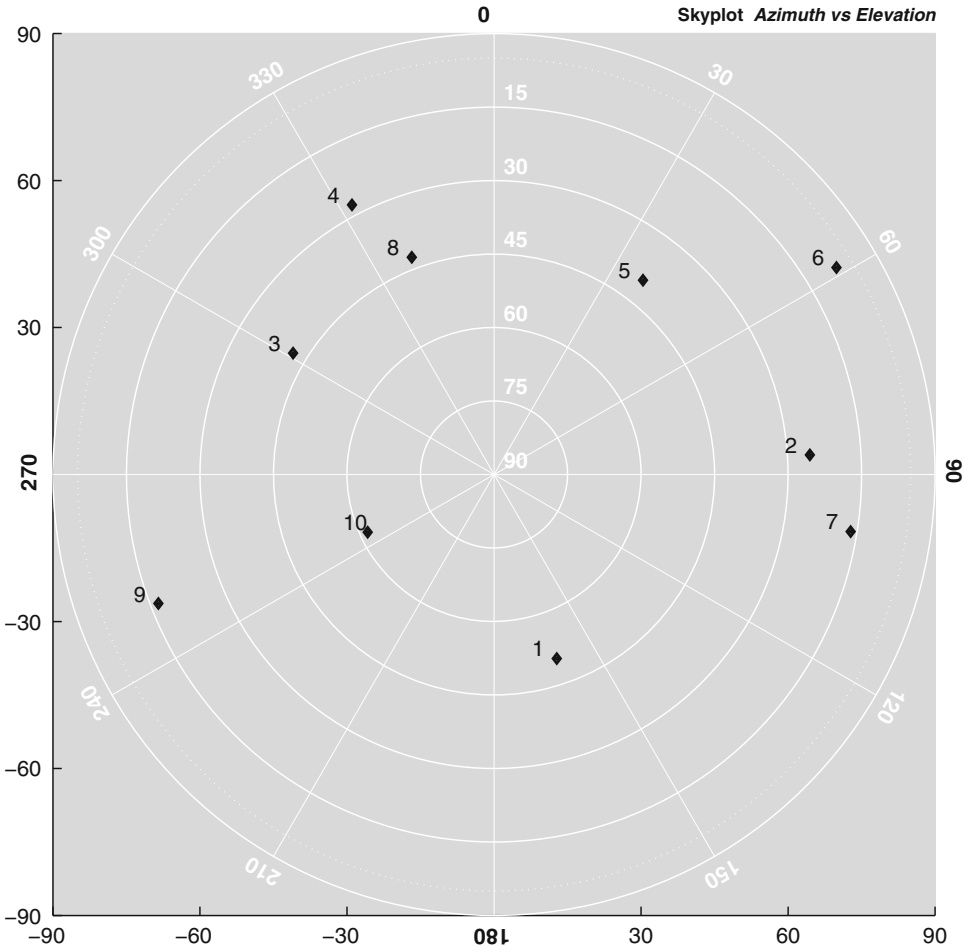

Fig. 1 GPS simulated constellation, skyplot

The same interpretation applies to the corresponding ratio τ between BNRs, given in Table 3 as function of the number of satellites and channels. The improvement obtained by adopting the AC model is amplified with respect the MDBs ratio, with BNRs ratios as large as three for the weakest scenario. The impact of an undetected error in the parameter estimation is thus largely reduced when adopting the AC model.

The second case study focuses on a simulated Galileo constellation. Galileo signals are more precise than GPS signals (cfr. Table 1), and will generally provide smaller absolute values for the MDBs and BNRs. However, we analyze here the relative performance between the UC and AC models, rather than the absolute improvement obtained by employing more precise observations.

Tables 4 and 5 reports the ratios between MDBs and BNRs for the Galileo scenario, relative to the detectability of an outlier on the third receiver, first observation at frequency L5. The larger gain associated to the AC model is again obtained in weaker scenarios, when limited number of satellites and/or single-frequency observations are available, with MDBs twice as large and BNRs three times as large when using the UC model. The extent of the improvement is then comparable to the one of the GPS case study, although with slight differences due to the satellite geometry and to the different accuracy between signals within the same GNSS.

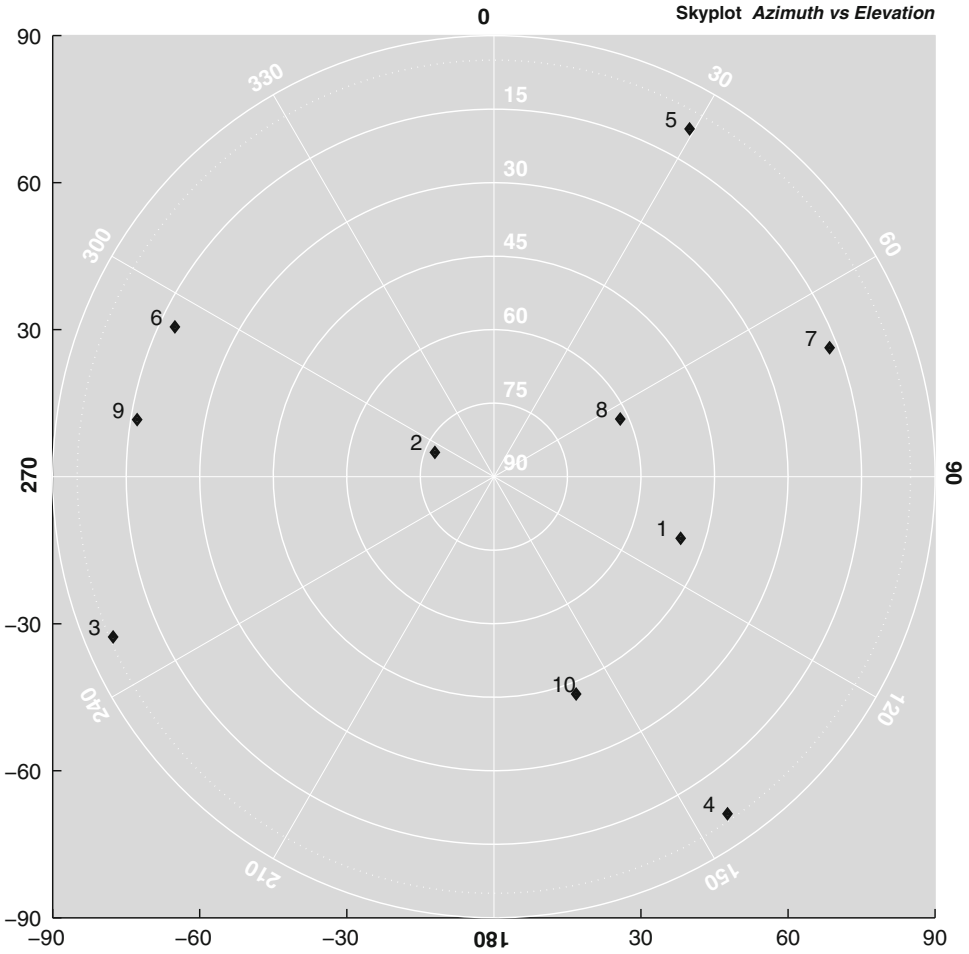

Fig. 2 Galileo simulated constellation, skyplot

Table 2 Ratio ω for GPS-only satellites, as function of number of satellites and frequencies available

# sat	L5	L1 + L5	L2 + L5	L1 + L2 + L5
4	–	1.58	1.58	1.32
5	2.06	1.38	1.38	1.24
6	1.10	1.07	1.07	1.05
7	1.06	1.04	1.04	1.03
8	1.06	1.04	1.04	1.03
9	1.06	1.04	1.04	1.03
19	1.06	1.04	1.04	1.03

The ratio ω refers to the detectability of an outlier on the third receiver, first observation at frequency L5

Table 3 Ratio τ for GPS-only satellites, as function of number of satellites and frequencies available

# sat	L5	L1 + L5	L2 + L5	L1 + L2 + L5
4	–	2.31	2.31	1.93
5	3.02	2.03	2.03	1.81
6	1.61	1.56	1.56	1.54
7	1.55	1.52	1.52	1.51
8	1.55	1.53	1.53	1.51
9	1.55	1.52	1.52	1.51
10	1.55	1.52	1.52	1.51

The ratio τ refers to the presence of an outlier on the third receiver, first observation at frequency L5

Overall, the strengthening of the observation model obtained by imposing linear constraints yields an effective reduction of the MDBs and BNRs, thus proving the advantage of affine-constrained models in terms of reliability for those configurations of antennas whose relative positions can be modeled as spatially invariant.

Table 4 Ratio ω for Galileo-only satellites, as function of number of satellites and frequencies available

# sat	E5	E1 + E5	E5a + E5	E1 + E5 +E6	E5a + E5b +E5 + E6	E1 + E5a +E5 + E6
4	–	2.32	1.86	1.60	1.35	1.40
5	1.44	1.34	1.28	1.24	1.17	1.18
6	1.34	1.27	1.23	1.20	1.14	1.15
7	1.35	1.28	1.24	1.20	1.14	1.16
8	1.17	1.14	1.13	1.11	1.09	1.09
9	1.16	1.14	1.12	1.11	1.08	1.09
10	1.14	1.12	1.11	1.09	1.07	1.08

The ratio ω refers to the detectability of an outlier on the third receiver, first observation at frequency E5

Table 5 Ratio τ for Galileo-only satellites, as function of number of satellites and frequencies available

# sat	E5	E1 + E5	E5a + E5	E1 + E5 +E6	E5a + E5b +E5 + E6	E1 + E5a +E5 + E6
4	–	3.39	2.72	2.34	1.97	2.05
5	2.11	1.95	1.88	1.81	1.71	1.73
6	1.96	1.85	1.80	1.75	1.67	1.69
7	1.98	1.87	1.81	1.76	1.68	1.69
8	1.72	1.68	1.65	1.63	1.59	1.60
9	1.70	1.67	1.64	1.62	1.58	1.59
10	1.67	1.64	1.62	1.60	1.57	1.58

The ratio τ refers to the detectability of an outlier on the third receiver, first observation at frequency E5

5 Conclusions

In linear models, linear constraints on parameter subsets potentially enable improved error detection, thanks to an implicit enhanced observations-to-unknowns redundancy. A consistent improvement in terms of integrity properties can be obtained by adopting the affine-constrained model over the unconstrained formulation. The improvement was captured analytically by expressing the ratio between minimum detectable biases (and bias-to-noise ratios) obtained in the linearly-constrained and unconstrained models.

The theorem finds a direct application in arrays of GNSS antennas whose relative distances do not vary. Following a re-parameterization of the baseline coordinates in terms of an attitude matrix, the observation model becomes linearly constrained when disregarding the orthonormality of the attitude matrix. The GNSS attitude model with affine constraints yields enhanced internal and external reliability, as demonstrated with several numerical examples that provide evidence of the improved performance of the affine-constrained model in terms of minimum detectable biases and bias-to-noise ratios.

Acknowledgements The research of Peter J.G. Teunissen has been supported by an Australian Research Council Federation Fellowship (project number FF0883188).

References

Baarda W (1968) A testing procedure for use in geodetic networks. Netherlands Geodetic Commission Publications on Geodesy, vol. 2, issue 5, 97 p

Bar-Itzhack IY, Montgomery P, Garrick J (1998) Algorithm for attitude determination using global positioning system. J Guid Control Dyn 21(6):846–852

Cohen CE (1992) Attitude determination using GPS. Ph.D. Thesis, Stanford University, Palo Alto, CA

Giorgi G (2011) GNSS carrier phase-based attitude determination. Estimation and applications. Delft University of Technology

Giorgi G, Teunissen PJG (2013) Low-complexity instantaneous ambiguity resolution with the affine-constrained GNSS attitude model. IEEE Trans Aerosp Electron Syst 49(3):1745–1759

Giorgi G, Teunissen PJG, Verhagen S, Buist PJ (2011) Instantaneous ambiguity resolution in GNSS-based attitude determination applications: the MC-LAMBDA method. J Guid Control Dyn 35(1):51–67

Giorgi G, Teunissen PJG, Verhagen S, Buist PJ (2012) Integer ambiguity resolution with nonlinear geometrical constraints. IAG Symp 137:39–45

Shuster MD (1993) A survey of attitude representations . J Astronaut Sci 41(4):439–517

Strang G, Borre K (1997) Linear algebra, geodesy, and GP. Wellesley-Cambridge Press, Welleseley

Teunissen PJG (1993) Least squares estimation of the integer GPS ambiguities. Invited lecture, Section IV theory and methodology, IAG general meeting, Beijing also in: LGR series No 6, Delft Geodetic Computing Center, Delft University of Technology

Teunissen PJG (1999) An optimality property of the integer least-squares estimator. J Geod 73(11):587–593

Teunissen PJG (2006) Testing theory: an introduction. Series on mathematical geodesy and positioning, 2nd edn. Delft Academic Press, Orlando

Teunissen PJG (2007) A general multivariate formulation of the multi-antenna GNSS attitude determination problem. Artif Satell 42(2):97–111

Teunissen PJG (2012) The affine constrained GNSS attitude model and its multivariate integer least-squares solution. J Geod 86:547–563

Teunissen PJG, Kleusberg A (1998) GPS for geodesy, 2nd edn. Springer/Heidelberg, Berlin/New York